REVISTA MATÉRIA V.29 N.3
ISSN 1517-7076 articles e20240450, 2024

Mechanical properties of glass-fiber reinforced polyester composites manufactured by two different spray-up techniques

Germano Scarabeli Custódio Assunção[1], João Adelir Velasques[2], Alberto Zakrzevski[2], Isidoro de Costa[2]

[1]Centro Universitário UNIVEL, Núcleo de Estudos e Pesquisas em Engenharias. Avenida Tito Muffato, n. 2317, Cascavel, PR, Brasil.

[2]Mascarello Carrocerias e Ônibus Ltda. Rodovia BR 277, Km 601, Cascavel, PR, Brasil.

e-mail: germano.s.c.assuncao@gmail.com, fabrica.joaov@mascarello.com.br, engenharia.alberto@mascarello.com.br, ferramentaria.isidoro@mascarello.com.br

ABSTRACT

The study evaluates two methods for producing glass-fiber reinforced polyester (GFRP): the traditional spray-up process and a modified method named Resin Spraying with Vacuum Assisted Molding (RSVAM). Manufacturing processes for resin composites are briefly reviewed, with detailed description of RSVAM. Tensile, flexural, and Izod impact strength tests were conducted on GFRP samples containing 30 wt.% fiberglass from both methods. RSVAM yielded 120 samples (40 per test type), with results including average tensile strength (31 ± 3 MPa) and modulus (6.2 ± 0.2 GPa), flexural strength (157 ± 7 MPa) and modulus (7.2 ± 0.1 GPa), and Izod impact resistance (107 ± 2 J/cm). Comparison with 120 samples from the spray-up method revealed no significant difference in tensile and flexural strengths at a 5% significance level, but RSVAM samples showed 168% higher Izod impact resistance. Reliability curves, based on parametric and nonparametric statistics, predicted failure probabilities. For tensile and flexural tests, normal and Weibull distributions were analyzed, with similar outcomes favoring Weibull for flexural tests. Nonparametric analysis was suitable for Izod impact results, showing significant differences in failure probabilities between the two processes.

Keywords: Fiberglass; Polyester; Spray-up technique; Weibull distribution; Kernel density estimation.

1. INTRODUCTION

Fiberglass as a reinforcement of unsaturated polyester matrix has been used since the 40s for military applications and it is currently used in a variety of civilian applications, such as naval, automotive and aeronautical industries. These materials are largely used due to their superior strength, lightweight and adaptable design [1].

The first method applied to produce GFRP was the hand lay-up. However, as civil applications were growing, other conventional processes were developed. Nowadays, the most applied conventional processes to manufacture glass-fiber reinforced polyester are: (1) hand lay-up; (2) spray-up; (3) injection molding; (4) blow molding and (5) calendering and compression molding. As presented by LILA *et al.* [2], there are also a large variety of the so-called non-conventional ones, namely: (1) automated tape laying; (2) automated fiber placement; (3) automated stringer lamination; (4) vacuum assisted molding; (5) filament winding and (6) resin transfer molding.

However, as different approaches can lead to similar results, there is still no real consensus on the ideal pathway in determining an optimal design and manufacturing technique for a given application. Thus, it is common to encounter in the industry some derived methods, which present slight variations from those listed above in order to supply specific demands of time, costs, dimensional accuracy, mechanical properties and wastes produced. This trend has led many researchers and companies to deal with several new processes or process modifications.

GASCONS *et al.* [3] reviewed the most relevant techniques for fiber-reinforced polymer manufacture. Following the same path, ASIM *et al.* [4] presented a review of processes to produce hybrid polymer composites. DEVARAJU AND ALAGAR [5] studied the fabrication of fiber-reinforced unsaturated polyester composites, dividing those processes into two main groups: direct impregnation and indirect impregnation methods. Other comprehensive studies about manufacture processes to produce GFRP materials can be found in [6–11].

Corresponding Author: Germano Scarabeli Custódio Assunção Received on 16/07/2024 Accepted on 16/07/2024

DOI: https://doi.org/10.1590/1517-7076-RMAT-2024-0450

The mechanical properties of GFRP are as variable as manufacturing processes to produce them since it can change due to the manufacturing process itself; matrix-reinforcement ratio; orientation, size and arrangement of reinforcement; pressure and temperature along curing process, loading conditions, so forth. DAVALLO and PASDAR [12] compared mechanical properties of polyester containing 30 wt. (%) random glass-fiber formed by resin transfer molding mold(RTM) and hand lay-up techniques and concluded that both produce samples with similar flexural strength and flexural modulus of elasticity. DI BELLA *et al.* [13] evaluated the mechanical properties of glass/polyester sandwich structures under static conditions and concluded that a new lamination sequence and the use of a bonder at the interface skin/core improve the mechanical properties and reduce the micro-cracks start. ABDULLAH [14] studied two commercial types of reinforced glass fibers: chopped and 0/90 glass-fiber with unsaturated polyester resin and found that the random composite has tensile modulus, maximum stress, and yield strength higher than the 0/90 composites. BITTENCOURT *et al.* [15] compared the influence of three different GFRP manufacturing processes, namely, hand lay-up, vacuum hand lay-up, vacuum infusion, and concluded that the last one produced a material with better physical and chemical properties than the others. For instance, the tensile strength of vacuum infusion was 48.6% higher than the ones produced by the hand lay-up and 29.5% higher than the vacuum hand lay-up samples. Other examples of the influence of manufacturing conditions in mechanical properties of GFRP can be found into [16–19].

As explained by XIAO *et al.* [20], although the spray-up method is widely applied, there are not many studies and researches discussing its mechanical properties and manufacturing techniques. In fact, JACOB [21] had already presented observations concerning styrene emissions from the 'dirty' spray-up technique and the rebirth of a 'greener', cleaner and more versatile spray-up process. However, since then, not many advances have been made — it can partially be explained by the fact that several other manufacturing processes had been developed and become the focus of the researchers. Recently, ZIN *et al.* [22] proposed an automated spray-up process to produce vinyl ester resin composites reinforced with Pineapple Leaf Fibre (PALF)-glass, proposing a mass-production natural fiber composite process, in contrast to most of the current manually biocomposites fabrication methods. JEON *et al.* [23] studied how spray height, fiber content and fiber length can change fiber volume distribution and mechanical properties of chopped strands of glass fiber reinforced polymerized dicyclopentadiene.

In this context, the aim of the present work is twofold: (1) raise data about mechanical properties of spray-up manufacturing processes and (2) compare mechanical properties from samples produced by two different spray-up techniques — the well-known spray-up technique and a modified spray-up method proposed by ZAKRZEVSK *et al.* [24].

2. MANUFACTURING METHODS OF GLASS-FIBER REINFORCED POLYESTER

2.1. Hand lay-up

It was the first technique developed to manufacture GFRP composites. Also known as hand laminating, this method is still used to produce low-cost composites [3, 6, 7]. The process of manual lamination is based on placing several fiber reinforcements, which can be glass, aramid or carbon in a mold, and then apply resin on them, and with manual effort, distribute the resin in an uniform way on the fibers and wait for the final polymerization of the resin. It is considered as one of the simplest GFRP manufacturing processes, being carried out manually in open molds and does not require a large investment in specific equipment. Due to hand rolling, the quality of the final part is closely related to the ability of the operator. Thus operational training and technical conceptualization are important to obtain flawless parts. The few equipment required is low cost and easily found on the market, such as roller, brushes, container and solvents.

As claims GASCONS *et al.* [3], the major disadvantages of the hand lay-up process are health and safety considerations required in the workshop in order to protect the workers from the harmful styrene fumes emitted during the crosslinking of the resin during curing.

2.2. Spray-up

The spray-up (or spray lay-up) can be understood as a modified hand lay-up method since it includes the same prerequisites. In this technique, a spray gun is used to spray pressurized resin (unsaturated polyester is one of the most common) and reinforcement which is in the form of chopped fibers, which significantly speeds up the process. It is also a less expensive alternative because it starts from a raw low-processed material such as fiber reels, which represent a cheaper reinforcement constituent than carefully constructed reinforcement layers.

Chopped roving is continuously supplied into the spray-gun and mixed with resin (in a predetermined ratio), and the mixture is in turn sprayed onto the mold [9]. Air stream is used to feed the composites onto

the mold. Release gel (gel coat) is usually applied on to the mold surface to facilitate the easy removal of components from the mold. After simultaneous application of chopped roving and spray resin, directly on the mold surface, hand rolling is required to accommodate this compound to the mold profile, as well as to remove air bubbles. Accelerators and catalysts are frequently used and curing may be done at room temperature or at high temperatures.

The spray-up manufacturing process is usually used in the production of medium to large parts from simple profiles to the most complex ones. The spray-up process is much faster than the hand lay-up process and is a less expensive choice [13]. Continuous roving is the least expensive form of reinforcement, and a chopper gun is capable of laying down material very rapidly. However, although a faster technique than hand lay-up, the interaction between composite parts and the operators is still required. Concerns about operator's health have led to a continuous replacement of this technique by closed mold infusion techniques.

2.3. Vacuum infusion techniques

A large number of infusion methods are mentioned in literature and patents. Vacuum infusion is a term with many acronyms since many researchers and companies are focused on understanding and improving such techniques [10]. Basically, one of the most important characteristics of vacuum infusion methods is that there is a pressure difference between the resin supply and cavity caused by a vacuum pump. Fibers are laid dry into the mold and the vacuum is applied before introduction of resin. Once a complete vacuum is achieved, the pressure difference between resin reservoir and cavity is the driving force for the resin flow. This process is assisted by an assortment of supplies and materials. Figure 1 illustrates a typical vacuum infusion technique called Vacuum Assisted Resin Transfer Molding (VARTM), that has been used since the 1950s to manufacture fiber reinforced thermoset components [8].

Very large parts can be made by this method although it requires a very low viscosity resin and a relatively long fill time as well as bleeder film and other venting. The resin infusion process results in very low void content and excellent mechanical properties due to the relatively high glass fiber content. To more detail about this technique, HINDERSMANN [10] and VAN OOSTEROM *et al.* [11] present an overview of the most used infusion processes (and modification of existing ones), such as Resin Infusion under Flexible Tooling (RIFT), Vacuum Assisted Resin Infusion Molding (VARIM), Vacuum Resin Injection Molding (VRIM), Differential Pressure Resin Transfer Molding (DP-RTM) and Closed Cavity Bag Molding (CCBM).

2.4. Resin injection techniques

As explains HINDERSMANN [10], the principal difference between infusion and injection techniques is the tool design. The former uses flexible film (Figure 1) for the infusion process and the pressure in the cavity is lower than ambient pressure; the latter requires rigid mold and pressures higher than ambient. Thus, resin injection techniques can be classified as double-sided closed mold systems. The most preeminent example of this technique is the Resin Transfer Molding (RTM) method. In this method, a preform made of the desired fiber (carbon, glass, or aramid) is placed inside a mold, and liquid resin such as epoxy or polyester is injected into the mold by means of a pump [7] — resin injected into the mold using single or multiple inlet ports. Reinforcements can be stitched, but more commonly they are made into a preform that maintains its shape during injection of the polymer matrix.

This process is widely acceptable in various industries, and can be applied to large and complex shapes. Moreover, this process involves a closed mold, which reduces styrene emissions to a minimum value. In general, RTM produces much fewer emissions compared to hand layup or spray-up techniques. The works of TUSHER *et al.* [25] and PLUMMER *et al.* [26] bring details about this technique.

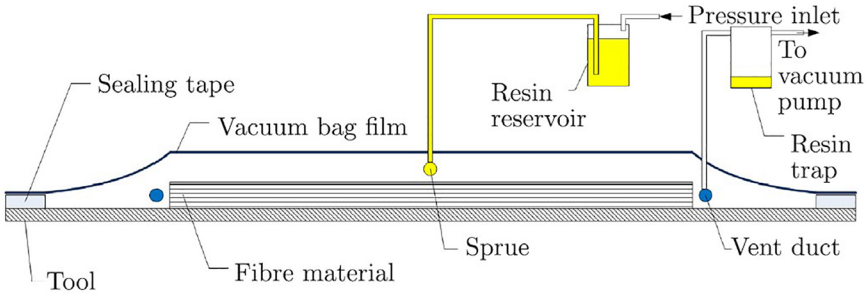

Figure 1: Schematic drawing of VARTM, modified from Hindersmann (2019).

2.5. Resin spray with vacuum assisted molding (RSVAM)

The process called here RSVAM was recently developed by ZAKRZEVSK *et al.* [24]. It had as main objectives: (1) improve productivity; (2) reduce costs of mass production bus body panels and (3) promote better working conditions for operators. This process was created by observing the positive characteristics presented by spray-up and closed-mold manufacturing processes. We highlight that ZAKRZEVSK *et al.* [24] proposed and described the method, but it was not named in their original work as RSVAM. We found such designation suitable based on process, as follows.

Firstly, a two-part mold dies must be made: Figure 2a illustrates a schematic cross-section view of the mold dies. The material used to produce those parts are GRFP with 10 mm (or superior) thickness manufactured from hand lay-up process using chopped strand mat 450 g/m^2 and unsaturated polyester (30:70 ratio). Figure 2b indicates a metal nozzle, where the vacuum suction is inserted to remove the air inside the mold cavity — a resin trap in a vacuum duct is required to protect the vacuum pump. Through the removal of this air using vacuum, the upper mold die (Figure 2c) is attached to the lower mold die (Figure 2d). Figure 2e illustrates rubber gaskets fastened in the upper mold die. It assures vacuum action in the internal cavity. The male mold die closes leaving a gap according to manufactured geometry, forming a sealed vacuum chamber.

Alignment dowels in Figure 2f assist the sealing process. For rectangular or squared mold dies, these dowels are asymmetrically positioned, in order to avoid operational mistakes. Figure 2g presents steel structure from upper, while Figure 2h from lower mold dies; it is used to guarantee dimensional quality in produced parts, otherwise, the entire structure could bend or warp. Figure 2i exemplifies an RSVAM sample. After the production of mold dies, the first step of the manufacturing process is the application of gel coats over the entire surface of the lower mold die. Then a mixture of resin and fibers are sprayed onto the upper surface of the lower mold die. Mold dies are closed and vacuum is applied. Then, it is driven to a composite curing oven, in order to anneal, dry and harden the material at 45 °C temperature during a required time (such value can vary accordingly to manufactured geometries). Finally, samples are demolded and a visual inspection is carried out.

This process guarantees excellent surface finishes on both sides, as well as good conformability in a quite faster way, because closed mold dies are applied. In a typical spray-up process only one side is in contact with mold die, while the other is free and therefore quality is dependent on the experience of workmen. RSVAM also reduces variability in the thickness of the layer since more control is achieved. In addition, the use of closed molds can reduce emissions of toxic fumes, which provides better working conditions for operators.

RSVAM was originally proposed to manufacture bus body internal and external panels, however, it shows to be promising to produce swimming pools, boat hulls, storage tanks and automotive parts.

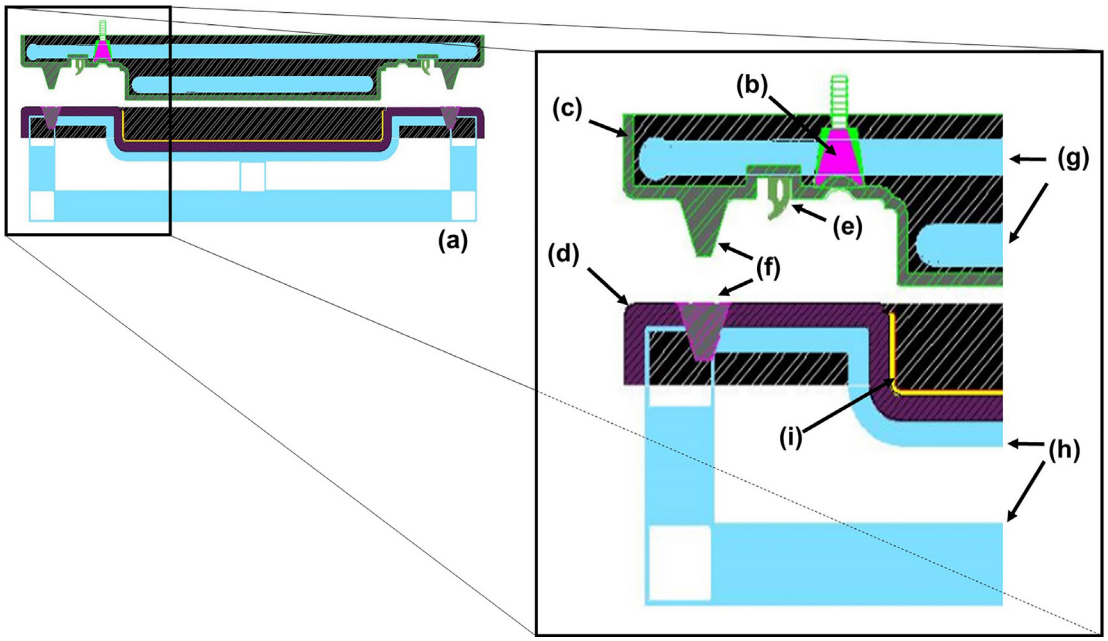

Figure 2: (a) schematic cross section view of RSVAM mold dies, (b) vacuum duct, (c) upper mold die, (d) lower mold die, (e) rubber gasket, (f) alignment dowels, (g) steel structure from upper mold die, (h) steel structure from lower mold die and (i) RSVAM sample.

3. MATERIALS AND METHODS

3.1. Specimens preparation

The materials used in this work were: (1) unsaturated polyester resin based on terephthalic acid (FORTCOM3100); (2) methyl ethyl ketone peroxide as a catalyst for curing resin (BRANOX® DM50-RED), (3) high performance sealer (Chemlease® 15 Sealer EZ); (4) wax-based release agent (Zyvax® Flex-Z™ 6.0); (5) orthophthalic gel coat supplied by Primus Compósitos; (6) assembled E-glass composite roving (Advantex® ME 3050S).

For both processes square GFRP mold dies (10 mm thick and 800 mm of length) were produced using the hand lay-up technique and following dimensions established by ASTM D638-14 [27], ASTM D790-17 [28] and ASTM D256-10R18 [29]. They were cleaned and their surfaces were coated with the sealer and the release agent. The gel coat was then evenly brushed over the mold die surface, to ensure the formation of a pure resin outer surface to the molding. After 15 minutes, the gel coat film with roughly 700-micron thickness has become stiff. Using a chopper gun, the glass-fiber was pulled out from a spool and automatically cut with 1.5 mm pieces. Then, the cut pieces were thrown into the catalyzed resin stream (1% catalyst per volume of resin). The resin and 30 wt. (%) of fiberglass were jointly sprayed directly onto the gel coat surface in the mold die to obtain samples with a thickness of 6.4 mm for flexural test and samples with a thickness of 3.2 mm for tensile and Izod impact tests. Fiber volume fraction was controlled following specifications defined by the equipment (Inter FLI-10) and to guarantee an accurate fiber volume ratio, we followed the following steps before manufacturing the samples tested: we collect only the applied resin for 30 seconds and we repeat the procedure with the fiberglass. After collecting both materials, we weighted them using a "Marte AD3300" precision balance (capacity up to 3000 g and readability down to 1 mg) in order to check the established ratio. Fiber volume fraction was measured before manufacturing samples from each method.

For traditional spray-up methods, air voids and the excess resin after spraying were released with a metallic roller from the open mold die. The samples were then cured in an oven for 30 minutes at (32 ± 3) °C and then post cured for 30 minutes at room temperature. After that, they were kept at room temperature for about 24 hours, then demolded. Finally, refined dimensions were manually obtained using cutting and sanding tools.

For the RSVAM method, after the joint application of resin and fiberglass onto the surface of the lower mold die, the upper mold die was placed over the lower one. Then vacuum was applied and trapped air was drawn, sealing the system and removing the excess resin/cut glass fibers. The closed mold was then driven to the oven and cured for 20 minutes at (42 ± 3) °C — the vacuum was maintained during this process. After completing the cure process, the vacuum source valve was closed and the vacuum vent was opened to vent the mold to atmospheric pressure, followed by a 30 minutes post-curing at room temperature. The mold dies were then opened and demolded after 24 hours. Again, the final dimensions were manually obtained using cutting and sanding machines.

3.2. Experimental procedure

Tensile properties of the produced GRRP were analyzed as suggests Test Method Type I, ASTM D638-14 [27]. As a whole, 80 specimens (40 from RSVAM and 40 from spray-up process) were manufactured. Universal testing machine WAW100-E (accuracy of 0.5% of measured load and load cell 100 kN) was used with a clip gauge extensometer with a gauge length of 50 mm (accuracy of 1% of measured extension) to obtain load-extension curve until fracture. The setup of the load-displacement measurement, including the clip gage extensometer, can be seen in Figure 3a. Speed of testing equal to 5 mm/min produced a rupture in approximately 3 min for specimen geometry used.

To evaluate flexural properties of a three-point bending test, 80 specimens were produced following recommendations of Procedure A, ASTM D790-17 [28] in a flatwise position. Beams of 127 mm (length) × 6,4 mm (width) × 3,2 mm (depth) were placed at support spans of 102 mm (support radius equal to 5 mm), which gave a support span-to-depth ratio of 16:1 and an overhanging on each end of roughly 12% of support span. Load until fracture of outer surface of the test specimen was applied midway (Figure 3b) between the supports with a rate of crosshead motion of 2.7 mm/min — calculated using Eq. (1). The same universal testing machine WAW100-E (accuracy of 0.5% of measured load) from the tensile standard test was applied. For each specimen tested, flexural stress, strain and modulus of elasticity were calculated through Eq. (2), (3) and Eq. (4), respectively:

$$R = \frac{ZL^2}{6d} \tag{1}$$

$$\sigma_f = \frac{3PL}{2bd^2} \tag{2}$$

$$\in_f = \frac{6Dd}{L^2} \tag{3}$$

$$E_B = \frac{L^3 m}{4bd^3} \tag{4}$$

where:

R: rate of crosshead motion (mm/min);

σ_f: stress in the outer fibers at midpoint (MPa);

$\in_f$: strain in the outer surface (mm/mm);

E_b: modulus of elasticity in bending (MPa);

D: maximum deflection of the center of the beam in a given point on the load-deflection curve (mm);

L: support span (mm);

P: load at a given point on the load-deflection curve (N);

Z: rate of straining of outer fiber. Based on Procedure A, ASTM D790-17 [28], Z = 0.01 (mm/mm/min);

b: width of beam tested (mm);

d: depth of beam tested (mm);

m: slope of the initial straight-line portion of the load-deflection curve (N/mm).

The Izod impact test to measure toughness of 80 specimens was applied based on Test Method A, ASTM D256-10R18 [29]. The specimens were cut to the required dimensions shown in Figure 4 (V notch of 45°prepared by a milling machine). Pantec Fit-300 was used to conduct the impact test. Reported values were calculated by dividing the absorbed energy values by the width of the specimen in cm, which gives the impact resistance under the notch in J/cm. Figure 3c illustrates the experimental setup for Izod standard test applied.

All the tests were carried out at room temperature of (22 ± 1) °C.

3.3. Statistical treatment

Composite materials are made from two or more constituent materials with significantly different mechanical properties. In GFRP, polyester forms a continuous phase (matrix), while glass-fibers the reinforcements (dispersion phase). For its nature, GFRP naturally can present different mechanical properties depending on several

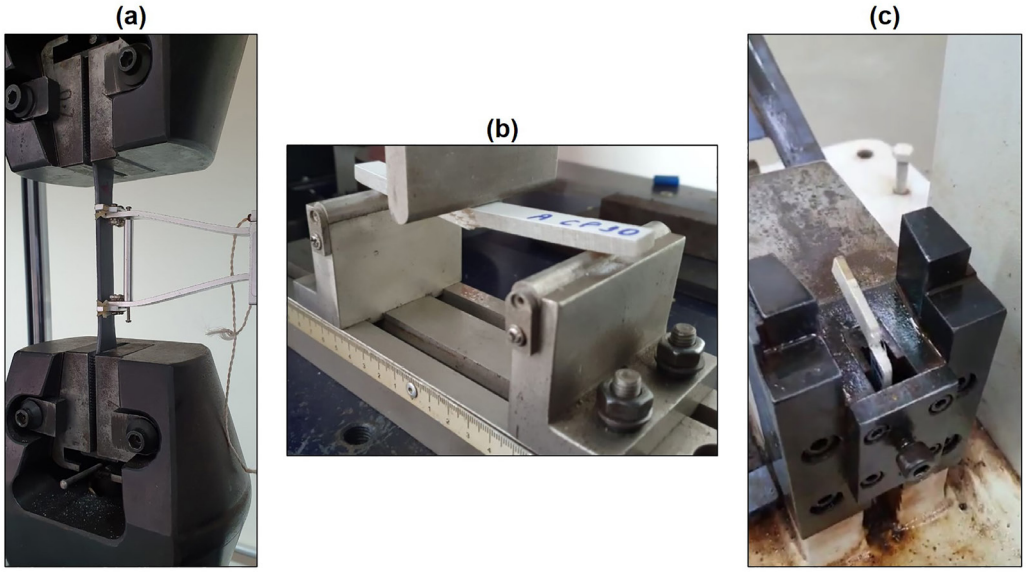

Figure 3: Experimental setup for (a) tensile, (b) flexural and (c) Izod impact standard tests.

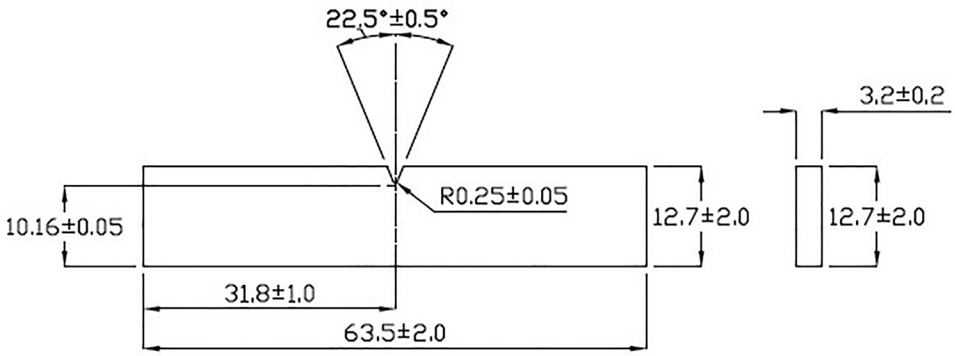

Figure 4: Dimensions of Type A specimens from Izod impact standard test.

parameters, such as: (1) manufactured process; (2) composition of reinforcement and (3) interfacial interactions established. In addition to this, they can present varying properties due to their internal structure since a series of internal defects can act as stress concentrating elements and that determine the points where the fracture of the product starts. As explained by MENEGAZZO *et al.* [30], the mechanical characteristics of a material depend on its microstructure and, mainly, on the distribution and size of the defects presented. As this distribution is almost always random, mechanical properties evaluated experimentally frequently show a large scattering in the measurement.

The three standard tests applied in the present work require a minimum of five specimens to determine the average values under study. However, due to the scatter in the measurements that composite materials can present, we can observe works with application of other statistical methods, instead of the calculation of a unique average value. Thus, we divided our analyses into two sections: (1) deterministic and (2) probabilistic. The first part follows recommendations presented in standard tests while the second one presents a more robust statistical study of tensile, flexural and toughness strengths.

3.3.1. Deterministic analysis: average value of fracture strengths

In this part, a straightforward method was used to evaluate stress-strain behavior on tensile and flexural tests, as well as the absorbed energy in the Izod impact test. We used tensile stress-strain curves from the RSVAM and the spray-up samples to obtain an "average curve" for each sample. Based on these average curves, a toe compensation was visually performed (following recommendation of ASTM D638-14 [27] and ASTM D790-17 [28]) and from the remaining curve, the tensile modulus of elasticity was estimated from linear regression. A similar procedure was applied in flexural analysis. This specific step was not applied in data from the Izod impact test.

After that, based on each tensile stress-strain curve, we identified the maximum stress, which corresponds to the tensile strength. Thus, two vectors were obtained, one from RSVAM and the other from spray-up samples. We used those vectors to calculate the average tensile strength and the associated standard deviation. Moreover, a one-way analysis of variance (ANOVA) [31] was performed to determine whether the tensile strength from the RSVAM samples had a common mean to the spray-up samples. The null hypotheses for which both vector are equal were tested at the 5% significance level. As explained by GOULD and RYAN [31], the level of significance is a cutoff value that indicates "how confident" is the conclusion drawn about the null hypothesis regarding the sample. A significance level of 5% means that we are 95% confident that our statistical conclusions did not occur by chance [32]. There is some concern about the use of the 5% of significance level, as discussed in work of WASSERTEIN and LAZAR [33]. However, it is still largely applied and it was also used is this work.

We applied the same methodological procedure in the flexural and toughness data-set. In addition, those vectors were input data in the probabilistic analysis of the following section.

3.3.2. Probabilistic analysis: application of parametric and nonparametric distributions

Generally, strength properties of composite materials are based on average values, as recommend by standards ASTM D638-14 [27], ASTM D790-17 [28] and ASTM D256-10R18 [29]. However, anisotropic behavior and misalignment of fiber direction during manufacturing process can scatter those properties, which can make the use of average strength values inaccurate to represent behavior of composite materials [34].

Due to this lack of homogeneity, employment of probabilistic approach provides a more rational and reliable framework for evaluating uncertainties of composite materials properties because instead of determine average values to represent scattered properties, we calculate "how likely a certain failure occurs", which gives probable scenarios for engineers and designers. Thus, they can decide what is the best decision in order to mitigate failure for a specific application.

To estimate the probability of failure, the steps usually taken are: (1) determination of distribution parameters from data-set available and (2) estimation of the cumulative distribution function, $F(x)$. Instead of $F(x)$, we can also find works that applied its complement, the reliability function $S(x) = 1 - F(x)$; in such cases the ones are interested in estimating the probability of material does not failure or "survival" applying reliability functions [34].

The first step, the determination of parameters, implies that the studied data-set can be described by a parametric distribution, such as normal, log-normal, gamma, Weibull or exponential. Parametric distributions are so called because assumes that data-set can be modeled by a fixed set of parameters. The most notable and applied parametric distribution for a variety of areas is the normal (or Gaussian) distribution [32], which are frequently used for random variables whose distributions are not know [35]. In this case, the mean ($\bar{\sigma}$) and the standard deviation (α) from measured values are the required parameters.

In the context of composite material science, the works of LU *et al.* [36] and WOLENSKI *et al.* [37] are some examples where normal distribution showed to be an accurate distribution to fit the data-set. In those cases, the cumulative distribution can be referred as $F(x; \bar{\sigma}, \alpha)$ and it is estimated by Eq. (5) [31]:

$$F(x;\ \bar{\sigma},\ \alpha) = \frac{1}{2}\left[1 + erf\left(\frac{\mathrm{x} - \bar{\sigma}}{\sqrt{2\alpha^2}}\right)\right] \tag{5}$$

Note that $F(x; \bar{\sigma}, \alpha)$ represents the probability that the fracture strength is equal or less than x, where the variable x is an value in MPa for tensile or flexural tests and in J/cm for Izod impact tests. Thus, if a certain value x is applied, the probability that the material will fail will be given by Eq. (5). As complement, the reliability function returns the probability that the fracture strength is at least x, that is, for a given value x, the probability that the material will not failure is given by Eq. (6) [31]:

$$S(x;\ \bar{\sigma},\ \alpha) = 1 - F(\mathrm{x},\ \bar{\sigma},\ \alpha) \tag{6}$$

Observe that $\bar{\sigma}$ and α are calculated from measured values from n samples, represented here by vector $\sigma = \{\sigma_1, \sigma_i \ldots, \sigma_n\}$. Both notations $F(x; \bar{\sigma}, \alpha)$ and $S(x; \bar{\sigma}, \alpha)$ are intentionally presented with normal parameters instead of only variable x, in order to highlight that we are assuming that for this case, σ follows a normal distribution.

Beyond normal distribution, over the last decades, Weibull distribution has been more used to describe the statistical properties of brittle and/or composites materials [35, 36], as this distribution as shown to be more accurate in predicting behavior of these materials. Examples with that application were shown in [30, 37–40].

In such case, Weibull scale parameter (σ_0) and Weibull shape parameter (m) must be determined instead of $\bar{\sigma}$ and α. The cumulative distribution function for Weibull distribution is then calculated by Eq. (7) [34]:

$$F(x;\ \sigma_0, m) = 1 - exp\left[-\left(\frac{x}{\sigma_0}\right)^m\right] \tag{7}$$

Where σ_0 is the characteristic stress at which the failure probability is 63.2%.

The associated reliability function can be computed by Eq. (8) [31]:

$$S(x;\ \sigma_0, m) = 1 - F(x;\ \sigma_0, m) \tag{8}$$

The two parameters applied in normal distribution are well-know and discussions about its calculation were suppressed of the presented work, but can be found in [31, 32]. However, the paths to estimate the two parameters from Weibull distribution are not straightforward.

To fit the Weibull distribution to the data and find Weibull scale and shape parameters used in Eq. (7) and (8), it is applied the linear regression based on maximum likelihood estimator from linear plot, shown in Eq. (9) [34].

$$In\left[In\left(\frac{1}{1-F(x;\ \sigma_0, m)}\right)\right] = m\ In\ x\ -\ m\ In\ \sigma_0 \tag{9}$$

Observe that $F(x; \sigma_0, m)$ is an unknown in Eq. (9), thus, it is estimated from measured values (σ), ordering the observations from smallest to largest. The estimates of $F(x; \sigma_0, m)$ are named here as $\hat{F}(\sigma_i; \sigma_0, m)$ and can be calculated by Hazen raking presented by Eq. (10) [41, 42]:

$$\hat{F}(\sigma_i;\ \sigma_0,\ m) = \frac{i-0.5}{n} \tag{10}$$

Where σ_i denote the ith observation from vector $\sigma = \{\sigma_1, \sigma_i \ldots, \sigma_n\}$ and $i = 1$ corresponds to the smallest and $i = n$ corresponds to the largest.

After plotting $\hat{F}(\sigma_i; \sigma_0, m)$ versus σ_i, it is possible to obtain m and σ_0. It is important to highlight that although there are other equations to calculate $\hat{F}(\sigma_i; \sigma_0, m)$, the one shown in Eq. (10) is widely used and is more accurate to estimate Weibull distribution, as concluded the works of KIRTAY and DISPINAR [42] and DAT-SIOU and OVEREND [43]. For this reason, it was applied in the present work.

Note that although both two-parameters distributions are widely used, it is not always applicable since we must to assume that measured samples follows a normal and/or a Weibull distribution. In order to check whether a sample of data comes from a population of specific distribution we must evaluate null hypothesis based on goodness-of-fit tests. In such cases, usually the null hypothesis is that the data-set follows a specific distribution and the goodness-of-fit tests will accept or reject that hypothesis. Whether the test accept the null hypothesis, we can conclude that normal and/or Weibull distributions are suitable to describe data-set used. To quantify that decision, we used a significance level of 5%, the same applied into deterministic approach.

There are several goodness-of-fit tests, such as Kolmogorov–Smirnov [44], Anderson–Darling (A-D test) [45] and Chi-square [46]. In this study we applied the A-D test to check the null hypothesis that measured samples are from a population with a normal/Weibull distribution. As explained by NOHUT [35], the A-D test can be understood as a modification of Kolmogorov–Smirnov test, but it has as advantage a more sensitive response to shape and scale of a distribution. There are several works that prove the accuracy of the A-D test [47–49] as much as applications of this test to study mechanic behavior of composite materials [37, 50].

Considering the scenario that the A-D test rejects the null hypothesis, another family of parametric distributions or a nonparametric analysis could be applied. Instead of test others parametric distributions, we decided to apply a nonparametric distribution, which can be used when some parametric distributions cannot properly describe the data-set. Although statistically accurate, a drawback of such approach is that there are not parameters to characterize the mechanical properties of tested materials, once this approach does not apply specific parameters to generate the cumulative distribution functions, such as the ones used in Eq. (5) and (7). A nonparametric distribution does not make assumptions about the data distribution, such as mean and standard deviations in normal method or shape and scale parameters in Weibull analysis. Most frequently nonparametric estimators are: histograms, empirical cumulative density function and kernel density estimators. Other available methods and further explanations about parametric and nonparametric methods are found into [31, 32, 51].

In this work, kernel density estimation (KDE) was used to generate the cumulative distribution function $F(x)$. KDE can be viewed as a smooth histogram and was initially proposed by ROSENBLATT [52]. For a given specific sample $\sigma = \{\sigma_1, \sigma_i \ldots, \sigma_n\}$ KDE estimates the probability density function $f(x)$ (formally referred as $\hat{f}(x)$) replacing the kernel function k in every element of the sample (σ_i). As shown in Eq. (11), $f(x)$ is then calculated as the sum of each kernel function [54]:

$$f(x) = \frac{1}{n}\sum_{i=1}^{n} k(x,\ \sigma_i;\ t) \tag{11}$$

where:

k: kernel function;

t: bandwidth, which is similar to the bin width in the histogram-based analysis.

As we can observe, kernel functions have a key hole in estimation of $f(x)$ because it is responsible for smoothing local data, making assumptions about neighborhood information. The most commonly used kernel functions are Gaussian kernel density estimator (k_G). In such cases, the kernel function can be calculated by Eq. (12) [53]:

$$k_G = (x,\ \sigma_i;\ t) = \frac{1}{\sqrt{2\pi t}} e^{-(x-\sigma_i)^2 \big/ (2t)} \tag{12}$$

BOTEV *et al.* [53] presented an alternative method to estimate kernel functions, where prior knowledge of the data is taken into account. They exploited the link between Gaussian kernel density estimator to Fourier heat equation and proposed a "KDE via diffusion" (diffusion referred in the well-known Fourier heat equation). Thus, for instance, if we know that a data set is nonnegative, this is taken into account, resulting in a more consistent estimate of the data. Eq. (13) summarizes ideas proposed by BOTEV *et al.* [53]:

$$k_b = (x,\ \sigma i;\ t) = \frac{1}{n} \sum_{k=-\infty}^{\infty} k(x,\ 2k - \sigma_i;\ t) + k(x,\ 2k - \sigma_i;\ t) \tag{13}$$

Where k_b represents the kernel function proposed by BOTEV *et al.* [53] and k can be formulated in different ways, depending of data analyzed. Thus, k in Eq. (13) can be understood as a "plug-in" to estimate k_b. Applying k_b in Eq. (11) and finally, integrating $f(x)$, we obtained $f(x)$. The cumulative distribution function was then applied to estimate the correspondent reliability function presented in Eq. (14) [31]:

$$S(x) = 1 - F(x) \tag{14}$$

Moreover, to determine whether average strengths from RSVAM are equal to spray-up samples when nonparametric method was applied, we used a nonparametric Wilcoxon rank sum test [31, 54] instead of one-way ANOVA [31], which is more recommend for not normally distributed samples [54].

It is important to highlight that that sample size affects directly the accuracy of both parametric and nonparametric distributions [54]. In this context, NOHUT [35] performed a study with 5100 experimental alumina strength data to investigate the effect of sample size on strength distributions and concluded that, at least 150-200 specimens should be used for the determination of the best fitting distribution function. Moreover, he showed that Weibull distribution usually best fits data with brittle behavior and at least 40 specimens must be used to guarantee Weibull parameters within an acceptable range. For this reason, 40 specimens were used in the present work.

We applied Matlab® to perform statistical analysis and generate reported graphics.

4. RESULTS

4.1. Tensile properties

As a whole 80 samples were test (40 for each manufacturing process). Specimens #7 and #8 from RSVAM, as well as #18 and #36 from spray-up broke outside of the narrow cross-sectional test section, therefore, they were discarded from the study, as recommend by ASTM D638-14 [27]. The remaining 38 specimens from both processes were used to evaluate tensile mechanical properties. As explains BITTENCOURT *et al.* [15], observed broke in the grip region can be explained by hand-tightening process, which causes preload. However, we highlight that the tightening process was performed carefully, in order to tight the grips evenly and firmly to prevent slippage of specimens. During the placement of the specimens, a special care was taken regarding alignment along the axis of the specimen and the grips with an imaginary line joining the points of attachment of the grips to the machine, as recommended by ASTM D638-14 [27].

We observed that fracture processes of all tested specimens were similar to the load-extension curve of specimen #5 in Figure 5a. To calculate tensile modulus, only linear region between load and extension shown in Figure 5b was considered.

Using the 38 load-extension curves from RSVAM, the average stress-strain curve presented in Figure 6a was obtained. After a visual toe compensation, linear regression ($R^2 = 0.99$) was applied and a tensile modulus of elasticity from RSVAM process was estimated in (6.2 ± 0.2) GPa. Figure 6b illustrates a similar method applied in spray-up samples, whose tensile modulus of elasticity was found (6.0 ± 0.2) GPa.

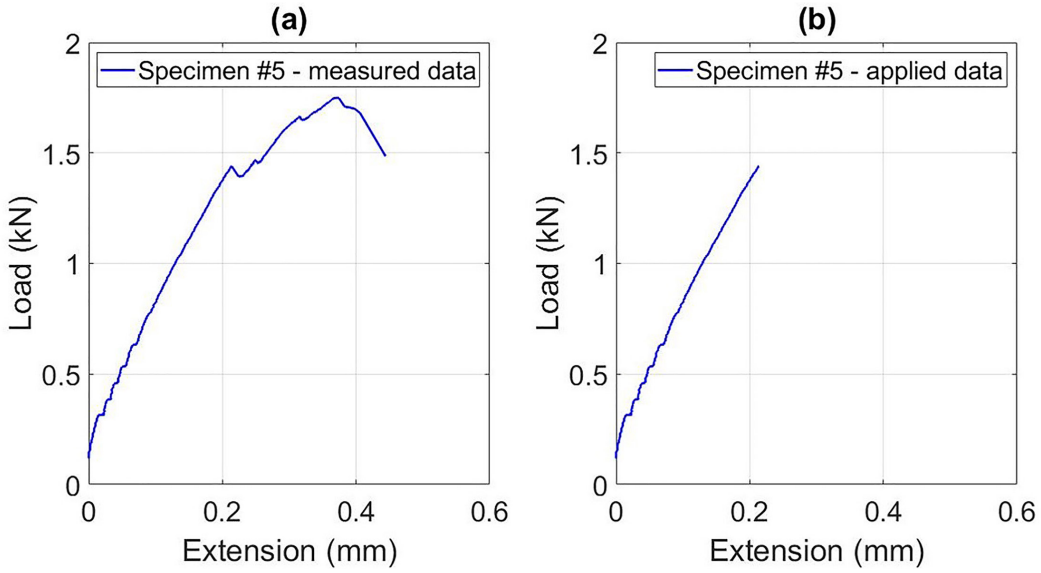

Figure 5: Load-extension curve for specimen #5 from RSVAM method during tensile standard test — (a) measured values until failure and (b) linear region used to calculate tensile modulus of elasticity.

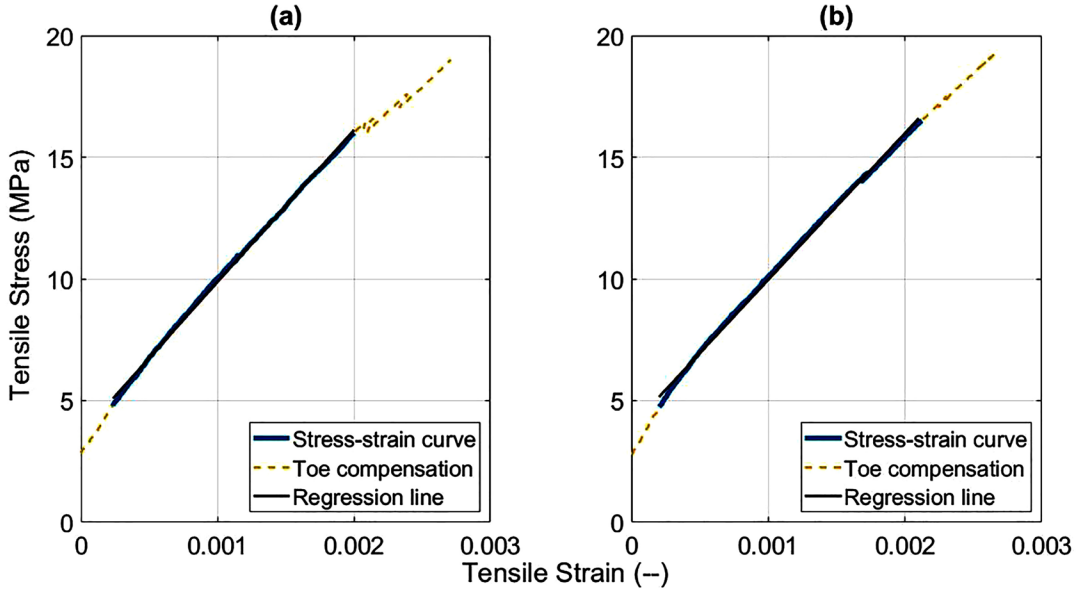

Figure 6: Stress-strain curve highlighting toe compensation and regression line for (a) RSVAM and (b) spray-up.

Based on ultimate load measured for each specimen, we calculated the average tensile strength for RSVAM sample as 31.1 MPa with a standard deviation of 11 MPa. A similar result was found from spray-up sample: 30.6 MPa and standard deviation of 9.3 MPa. ANOVA fails to reject the null hypothesis at 5% of significant level ($p = 0.8385$). Therefore, we conclude that both samples have a common average.

The a-D test showed that both samples can be described by populations of normal and Weibull distributions — respective p-values from the A-D test are shown in the legend of the Figure 7. Therefore, a parametric analysis was applied for both samples. Figure 7 presents the reliability curves obtained. As we can observe, 50% failure probability was the same, 31 MPa. From an overall perspective, we can conclude that both processes produced materials with similar tensile mechanical properties, and applications of the normal or Weibull distribution did not significantly affect conclusions drawn. Table 1 presents Weibull's scale and shape parameters estimated.

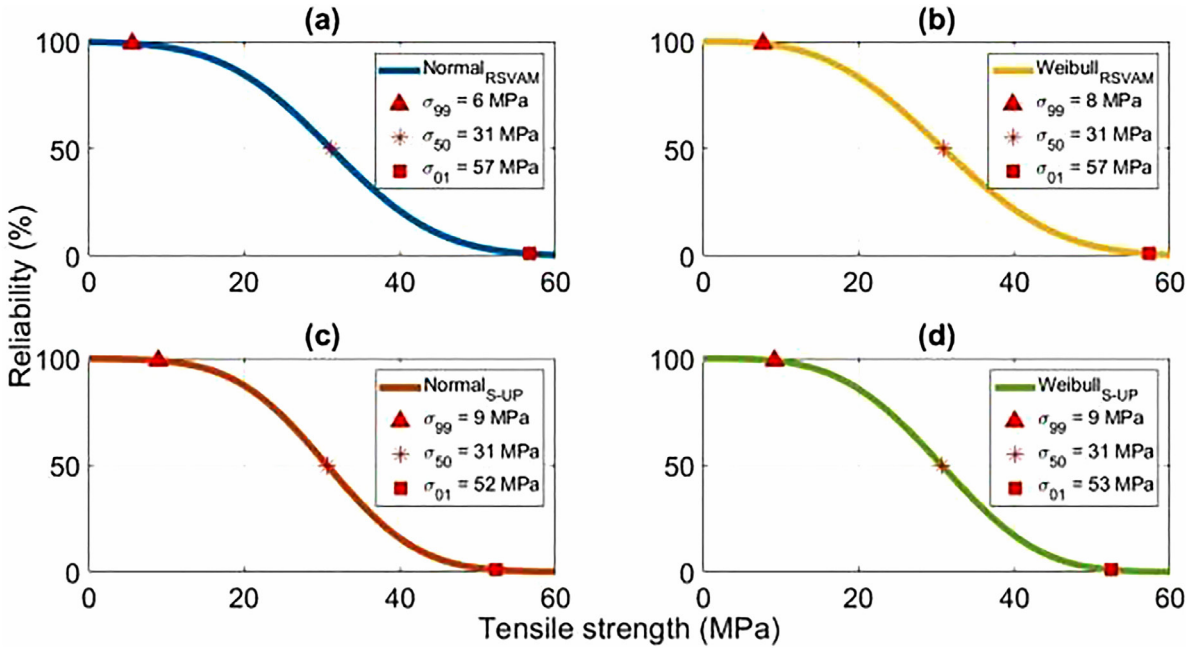

Figure 7: Reliability curves of tensile test for (a) RSVAM for normal distribution — p = 0.0787, (b) RSVAM for Weibull distribution — p = 0.3483, (c) spray-up for normal distribution — p = 0.4298, (d) spray-up for Weibull distribution — p = 0.0882.

4.2. Flexural properties

For flexural analysis, 40 stress-strain curves were obtained for RSVAM (Figure 8a) and other 40 curves for spray-up samples (Figure 8b). These curves were obtained by calculating stress and strain via Eq. (2) and (3), respectively. Based on these values, average stress-strain curves shown in Figures 8c and 8d were calculated. From a visual comparison, we can conclude that both processes produced materials with the same flexural stress-strain trend.

We used the slope from a linear regression (R^2 = 0.99) of average load-deflection curves and applied Eq. (4), obtaining flexural modulus of elasticity equal to (7.2 ± 0.1) GPa and (7.0 ± 0.1) GPa for RSVAM and spray-up, respectively. Considering the estimated errors, we concluded that the flexural modulus is the same for both.

The A-D test showed that both samples can be described by normal and Weibull distributions — respective p-values from the A-D test are shown in the legend of the Figure 9. Thus, a parametric analysis was applied. Using the ultimate load measured for each specimen, flexural strength for RSVAM was 157 MPa with a standard deviation of 21 MPa. A similar result was found from a spray-up sample: 155 MPa and a standard deviation of 22 MPa. From ANOVA we concluded that they have a common average since it fails to reject null hypothesis (p = 0.7807).

Figure 9 presents the reliability curves obtained, considering normal and Weibull approaches. As a whole, Weibull distributions showed more conservative estimates for 1% and 99% probability of failure, thus, to guarantee survival of the materials used in this work during flexural stress, the Weibull distribution seems to be the most suitable method. Weibull parameters calculated to generate curves Figures 9b and 9d are shown in Table 1.

4.3. Izod impact resistance

After application of Izod impact test, we observed that all the specimens separated into two pieces. Thus category C (complete break) was applied [29]. The A-D test rejects null hypothesis that RSVAM sample is from a normal distribution (p = 0.0201), while failed to reject Weibull distribution (p = 0.1438). From the spray-up samples, the converse was observed: the A-D test failed to reject that spray-up samples are from normal distribution (p = 0.0967) and reject the Weibull distribution null hypotheses (p = 0.0163).

In this scenario, considering limitations regarding the application of parametric statistics, since we cannot use normal distribution in RSVAM nor Weibull distribution in spray-up data-set, we adopted the nonparametric analysis.

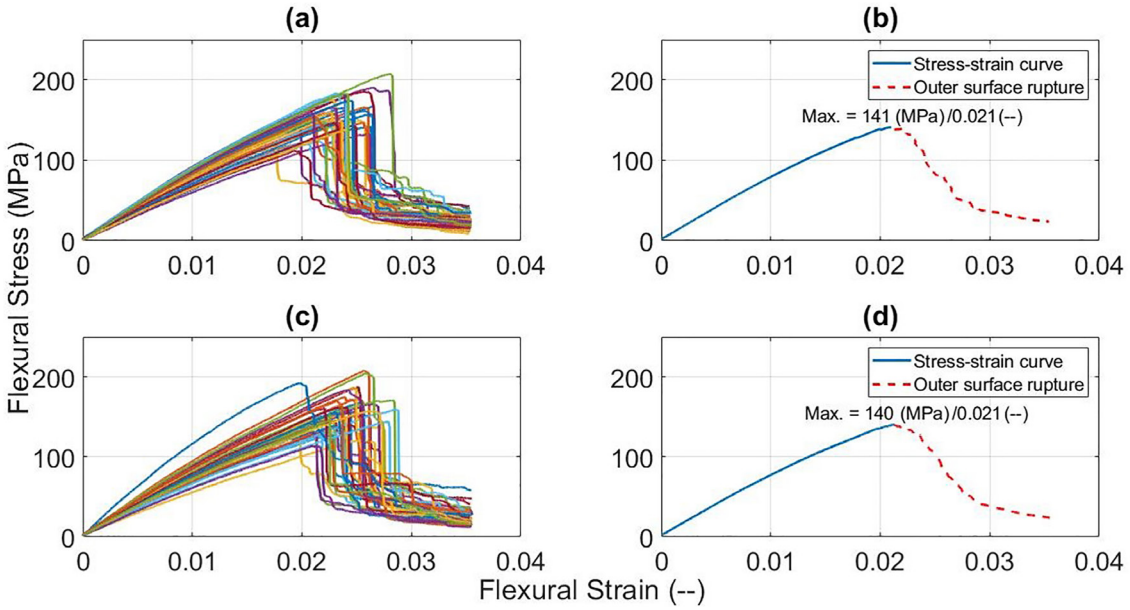

Figure 8: Stress-strain curves (a) RSAM and (b) Spray-up; Average stress-strain curves (c) RSVAM and (d) spray-up.

Table 1: Summary of scale and shape parameters for Weibull distributions.

STANDARD TEST	DESCRIPTION	RSVAM	SPRAY-UP
Tensile	Scale parameter (95% confidence interval)	34.8 (31.0 — 39.0)	34.0 (30.8 — 37.6)
	Shape parameter (95% confidence interval)	3.1 (2.4 — 3.9)	3.5 (2.8 — 4.5)
Flexural	Scale parameter (95% confidence interval)	165.9 (159.4 – 172.7)	165.2 (157.9 – 172.8)
	Shape parameter (95% confidence interval)	8.2 (6.5 – 10.3)	7.3 (5.8 – 9.1)

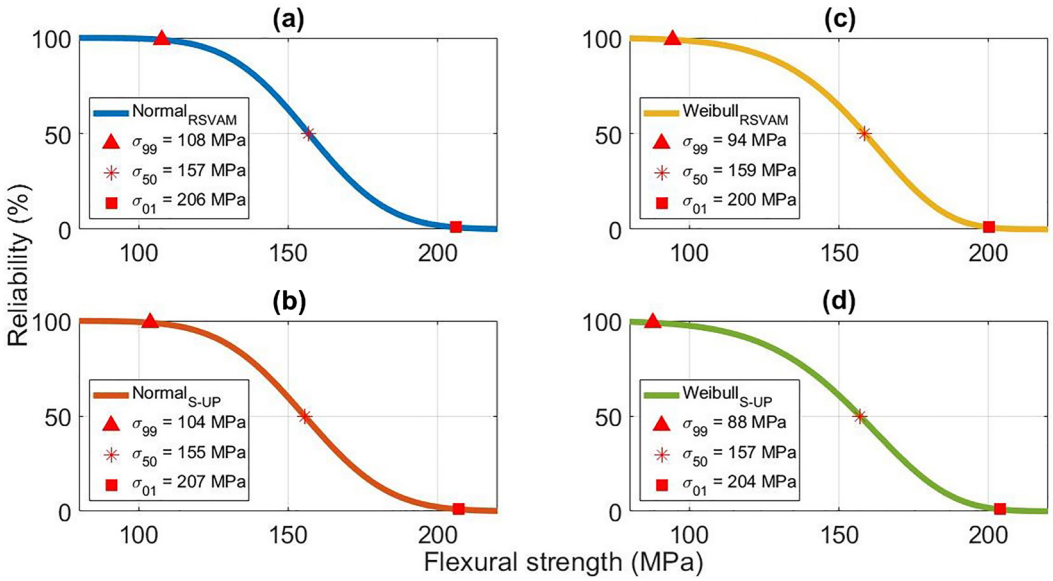

Figure 9: Reliability curves of flexural test for (a) Normal distribution (p = 0.8965) of RSVAM samples, (b) Normal distribution (p = 0.5562) of spray-up samples, (c) Weibull distribution (p = 0.5308) of RSVAM samples, (d) Weibull distribution (p = 0.0684) of spray-up samples.

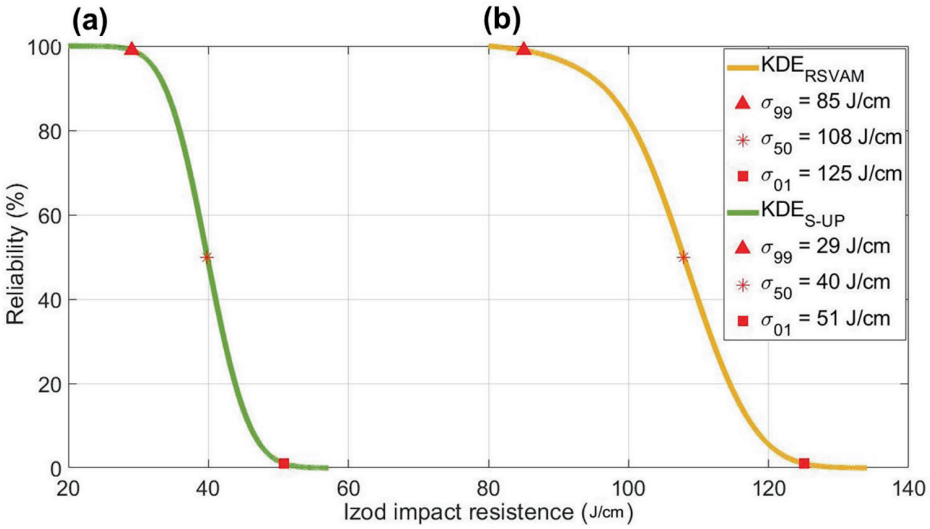

Figure 10: Reliability curves of flexural test from (a) RSVAM and (b) spray-up using KDE.

Instead of application of ANOVA, in this case we applied the nonparametric method Wilcoxon rank sum test, that rejected null hypotheses that both samples are from continuous distributions with equal medians ($p \approx 0.00$). In fact, significant differences were observed in Izod impact resistance. The sample from RSVAM method showed an average value of 107 J/cm with a standard deviation of 6.3 J/cm, while spray-up method presented an average of 39.9 J/cm and standard deviation of 2.8 J/cm. Thus, based on average values, the RSVAM method presented a resistance 168% greater than spray-up.

In the reliability curves generated from KDE proposed by BOTEV *et al.* [53], considerable visual differences can also be noticed, as shows Figure 10. In comparison to the tensile and flexural reliability curves, scatter of the data was lower in Izod impact resistance, producing more shrinking curves towards the average values.

5. DISCUSSION

Table 2 summarizes tensile properties obtained for RSVAM and spray-up techniques. Observing tensile strength and modulus of elasticity we can conclude that both processes produced samples without a significant difference for practical purposes. In fact, as previously discussed, one-way ANOVA fails to reject the null hypothesis that both samples have the same average (at 5% of significant level). Moreover, observing Figure 7, we can also conclude that the application of normal or Weibull distributions generate similar reliability curves.

ARAUJO *et al.* [55] reported an average tensile strength of (41.9 ± 0.9) MPa for 30 wt. (%) fiberglass/polyester composite material produced by hand lay-up process, while BRENES-ACOSTA and STRADI-GRANADOS [56] found average values equal to (87.3 ± 4.9) MPa and ISLAM *et al.* [19] 65 MPa[1]. Those results are greater than the average values presented in Table 2. Results from [19, 46] are even greater than the failure probability of 99% shown in Figure 7. Thus, we can conclude that hand lay-up technique produced materials with a better tensile strength than both spray-up techniques here presented, which can be expected, since hand lay-up processes normally use long fibers. The work of DEBNATH and SINGH [57] had already drawn a conclusion about higher tensile strength of hand lay-up method over than traditional spray-up method.

Regarding tensile modulus of elasticity, ARAUJO *et al.* [55], BRENES-ACOSTA and STRADI-GRANADOS [56], ISLAM *et al.* [19] obtained for similar composite materials manufactured using hand lay-up process values equal to (2.5 ± 0.5) GPa, (5.5 ± 0.2) GPa and 3.5 GPa, respectively, which are lower than the observed values from RSVAM and spray-up processes. Thus, regarding these results of the tensile modulus of elasticity, we can conclude that fiberglass/polyester materials produced via hand lay-up tend to have lower tensile modulus than spray-up materials.

Note that hand lay-up values were used as a benchmark, due to the lack of reported values of the spray-up process in the literature for polyester reinforced with 30 wt. (%) of fiberglass. We can find results such as those

[1] In the present work, values without errors were obtained from graphics with reported errors that cannot precisely be determined. For this reason, they were left without errors presented in the original papers.

presented in [7, 9, 15, 20, 22, 23, 58, 59], however, resin/reinforcement material or ratio are different from those used in this work.

Table 3 summarizes flexural properties obtained for RSVAM and spray-up techniques. EL-WAZERY *et al.* [17], ISLAM *et al.* [19] and DAVALLO and PASDAR [12] encountered lower average values for similar composites produced by hand lay-up process: 83 MPa, 75 MPa and (106 ± 3) MPa. Observing the reliability curves in Figure 9, results from [17] and [19] are even lower than failure probability of 1% considering normal and Weibull distributions obtained from RSVAM and spray-up specimens studied, while result from DAVALLO and PASDAR [12] is lower than the failure probability of 1% for normal analysis. BRENES-ACOSTA AND STRADI-GRANADOS [56] reported an average value of (155 ± 20) GPa for similar composite (also produced via hand lay-up), which is pretty similar to the ones found the present work, as showed Table 3.

Thus, taking into account average results, we can conclude that RSVAM and spray-up techniques produce materials with a similar flexural strength in comparison to each other; however, they present a superior flexural strength than similar composites produced through hand lay-up process.

Moreover, application of the reliability curves generated from Weibull distributions brought more conservative results than normal ones since the former stretched out the curves from RSVAM and spray-up to values lower than average. As an example, we can conclude that 1% of the samples from RSVAM will fail if a flexural tension lower than 94 MPa is applied (Figure 9c), while samples from spray-up fail at 88 MPa (Figure 9d). These values are lower than the ones observed for reliability curves from normal distributions (Figures 9a and 9b).

Therefore, from a perspective of flexural strength analysis, we recommend applications of the reliability curves from the Weibull distributions. Note that this is a suggestion of the application of reliability curves from Weibull analyses and not Weibull parameters themselves. As presents AFFERRANTE *et al.* [60], although largely used in failure analysis, Weibull module does not correspond to a material property, as it is often presented. Weibull's modulus can vary significantly, even for the same material, due to the interaction between the cracks and the stress field. Thus, as presented by them, using the Weibull module as a parameter similar to the Young modulus for ductile materials would be a gross simplification of the reality observed in fragile fractures.

Regarding flexural modulus of elasticity, ISLAM *et al.* [19] reported flexural modulus of elasticity of approximately 2.3 GPa for similar material produced from the hand lay-up process, which is significantly lower than the observed values of the present work (Table 3). MALLICK [59] reported the flexural modulus for polyester resins as 4.34 GPa, which is lower than the calculated values in the present work — it was an expected result, since glass fiber has a function of increase elastic moduli.

Table 2: Summary of tensile standard test.

PROPERTY	DESCRIPTION	RSVAM	SPRAY-UP
Number of specimens	–	38	38
Tensile strength	Average (stand. deviation)	31.1 (11) MPa	30.6 (9.3) MPa
	(Maximum value ± error)	(62 ± 2) MPa	(55 ± 2) MPa
	(Minimum value ± error)	(10.3 ± 0.5) MPa	(16.4 ± 0.7) MPa
Tensile modulus of elasticity	(Linear regression ± error)	(6.20 ± 0.02) GPa	(6.03 ± 0.02) GPa

Table 3: Summary of flexural strength values.

PROPERTY	DESCRIPTION	RSVAM	SPRAY-UP
Number of specimens	–	40	40
Flexural strength	Average (stand. deviation)	157 (21) MPa	155 (22) MPa
	(Maximum value ± error)	(207 ± 2) MPa	(208 ± 2) MPa
	(Minimum value ± error)	(112 ± 0.5) MPa	(114 ± 1) MPa
Flexural modulus of elasticity	(Linear regression ± error)	(7.2 ± 0.1) GPa	(7.0 ± 0.1) GPa

Regarding Izod impact resistance, we observed a significant improvement in this property comparing RSVAM to spray-up processes since RSVAM produced samples with average values 168% more resistant than spray-up methods. The main reason for this difference could be due to the vacuum and closed-mold system in RSVAM process, which improved accommodation of produced materials. Further analysis must be performed using photomicrographs to prove this claim.

6. CONCLUSIONS

A modification in spray-up method was described in the present work to manufacture glass-fiber/polyester composite materials in a faster and safer manner. Instead of performing hand rolling to accommodate composite material into mold profile and remove air bubbles, vacuum in a two-part mold system was applied. Such change improved the quality control, surface finish, while reduced the dry-cure time and exposure of operators to toxic fumes.

We compared the behavior of samples from tensile, flexural and Izod impact tests against to same quantity produced from spray-up method, used as a benchmark. Although manufacturing time has been reduced, we showed, at the 5% significance level, that tensile and flexural strengths from both processes have a common average. Moreover, the RSVAM increased the Izod impact resistance 168% in comparison to the spray-up method.

7. ACKNOWLEDGMENTS

The authors would like to thank the following institutions for supporting this work: Mascarello Carrocerias e Ônibus Ltda. and Centro Universitario UNIVEL. The authors also acknowledge technician Filipe de Carvallho Bernardino from Universidade Tecnológica Federal do Paraná (UTFPR) for assistance in conduction of standard tests and Dykenlove Marcelin for proofreading the article.

8. BIBLIOGRAPHY

[1] BADAWY, A.A.M., "Impact behavior of glass fibers reinforced composite laminates at different temperatures", *Ain Shams Engineering Journal*, v. 3, n. 2, pp. 105–111, 2012. doi: http://doi.org/10.1016/j.asej.2012.01.001.

[2] LILA, M.K., KOMAL, U.K., CHAITANYA, S., *et al*., "Secondary processing of polymer matrix composites: challenges and opportunities", In: *International Conference on Latest Development in Material, Manufacturing and Quality Control*, Bathinda, India, 2016.

[3] GASCONS, M., BLANCO, N., MATTHYS, K., "Evolution of manufacturing processes for fiber-reinforced thermoset tanks, vessels, and silos: a review", *IIE Transactions*, v. 44, n. 6, pp. 476–489, 2012. doi: http://doi.org/10.1080/0740817X.2011.590177.

[4] ASIM, M., JAWAID, M., SABA, N., *et al*., "Processing of hybrid polymer composites: a review", In: Thakur, V.K., Thakur, M.K., Gupta, R.K. (eds), *Hybrid polymer composite materials*, Duxford, UK, Woodhead Publishing, pp. 1–22, 2017.

[5] DEVARAJU, S., ALAGAR, M., "Unsaturated Polyester: macrocomposites", In: Thomas, S., Hosur, M. Chirayil, C.J. (eds), *Unsaturated Polyester Resins*, Oxford, UK, Elsevier, pp. 43–66, 2019.

[6] BHATT, A.T., GOHIL, P.P., CHAUDHARY, V., "Primary manufacturing processes for fiber reinforced composites: history, development & future research trends", *IOP Conference Series. Materials Science and Engineering*, v. 330, n. 1, pp. 012107, 2018. doi: http://doi.org/10.1088/1757-899X/330/1/012107.

[7] MAHBOUBIZADEH, S., SADEQ, A., ARZAQI, Z., *et al*., "Advancements in fiber-reinforced polymer (FRP) composites: an extensive review", *Discover Materials*, v. 4, n. 1, pp. 22, 2024.

[8] RICCIARDI, M.R., ANTONUCCI, V., DURANTE, M., *et al*., "A new cost-saving vacuum infusion process for fiber-reinforced composites: pulsed infusion", *Journal of Composite Materials*, v. 48, n. 11, pp. 1365–1373, 2014. doi: http://doi.org/10.1177/0021998313485998.

[9] SAPUAN, S.M., *Composite materials: concurrent engineering approach*, Oxford, Butterworth-Heinemann, 2017. doi: http://doi.org/10.1016/B978-0-12-802507-9.00003-9.

[10] HINDERSMANN, A., "Confusion about infusion: an overview of infusion processes", *Composites. Part A, Applied Science and Manufacturing*, v. 126, pp. 105583, 2019.

[11] VAN OOSTEROM, S., ALLEN, T., BATTLEY, M., *et al*., "An objective comparison of common vacuum assisted resin infusion processes", *Composites. Part A, Applied Science and Manufacturing*, v. 125, pp. 105528, 2019.

[12] DAVALLO, M., PASDAR, H., "Comparison of mechanical properties of glass-polyester composites formed by resin transfer molding and hand lay-up technique", *International Journal of Chemtech Research*, v. 1, n. 3, pp. 470–475, 2009.

[13] DI BELLA, G., BORSELLINO, C., CALABRESE, L., "Effects of manufacturing procedure on unsymmetrical sandwich structures under static load conditions", *Materials & Design*, v. 35, pp. 457–466, 2012.

[14] ABDULLAH, E.T., "A study of bending properties of unsaturated polyester/glass fiber reinforced composites", *Journal of Al-Nahrain University*, v. 16, n. 3, pp. 129–132, 2013. doi: http://doi.org/10.22401/JNUS.16.3.18.

[15] BITTENCOURT, A.P.P., DUTRA, G.B., TANCREDI, T.P., "Effects of lamination processes on the physical and mechanical properties of fiberglass/polyester composites", *Matéria (Rio de Janeiro)*, v. 21, n. 04, pp. 1021–1031, 2016. http://doi.org/10.1590/s1517-707620160004.0094.

[16] SHEN, R., LIU, T., LIU, H., *et al*., "An enhanced vacuum-assisted resin transfer molding process and its pressure effect on resin infusion behavior and composite material performance", *Polymers*, v. 16, n. 10, pp. 1386, 2024. doi: http://doi.org/10.3390/polym16101386. PubMed PMID: 38794579.

[17] EL-WAZERY, M.S., EL-ELAMY, M.I., ZOALFAKAR, S.H., "Mechanical properties of glass fiber reinforced polyester composites", *International Journal of Applied Science and Engineering*, v. 14, n. 3, pp. 121–131, 2017.

[18] HEMANTH, R.D., KUMAR, M.S., GOPINATH, A., *et al*., "Evaluation of mechanical properties of E-glass and coconut fiber reinforced with polyester and epoxy resin matrices", *International Journal of Mechanical and Production Engineering Research and Development*, v. 7, n. 5, pp. 13–20, 2017. doi: http://doi.org/10.24247/ijmperdoct20172.

[19] ISLAM, M.N., AR-RASHID, H., ISLAM, F., *et al*., "Fabrication and characterization of e-glass fiber reinforced unsaturated polyester resin based composite materials", *Nano Hybrids and Composites*, v. 24, pp. 1–7, 2019. doi: http://doi.org/10.4028/www.scientific.net/NHC.24.1.

[20] XIAO, B., YANG, Y., WU, X., *et al*., "Hybrid laminated composites molded by spray lay-up process", *Fibers and Polymers*, v. 16, pp. 1759–1765, 2015.

[21] JACOB, A., "Spray-up offers process improvements", *Reinforced Plastics*, v. 46, n. 1, pp. 32–36, 2002.

[22] ZIN, M.H., ABDAN, K., MAZLAN, N., *et al*., "Automated spray up process for Pineapple Leaf Fibre hybrid biocomposites", *Composites. Part B, Engineering*, v. 177, n. 15, pp. 107306, 2019. doi: http://doi.org/10.1016/j.compositesb.2019.107306.

[23] JEON, J.H.J., YOON, C.K., PARK, S.H., *et al*., "Assessment of long fiber spray-up molding of chopped glass fiber reinforced polydicyclopentadiene composites", *Fibers and Polymers*, v. 21, n. 5, pp. 1134–1141, 2020. doi: http://doi.org/10.1007/s12221-020-9676-3.

[24] ZAKRZEVSK, A., COSTA, I., VELAQUES, J.A., *Processo de produção de peças em plástico reforçado com fibra de vidro*. BR 10 2020 005411 2, 18 mar. 2020.

[25] TUSHER, M.H., IMAM, A., KHATUN, M.A., *Hybrid composite materials*, Singapore, Springer, 2024.

[26] PLUMMER, C.J.G., BOURBAN, P.E., MANSON, J.A., "Polymer matrix composites: matrices and processing", *Reference module in materials science and materials engineering*, Lausanne, Elsevier, pp.7388–7396, 2016. https://doi.org/10.1016/B978-0-12-803581-8.02386-9.

[27] ASTM INTERNATIONAL, *D638-14: Standard Test for Tensile Properties of Plastics*. West Conshohocken, American Society for Testing and Materials, 2022.

[28] ASTM INTERNATIONAL, *D790-17: Standard Test Method for Unreinforced and Reinforced Plastics and Electrical Insulating Materials*. West Conshohocken, American Society for Testing and Materials, 2017.

[29] ASTM INTERNATIONAL, *D256-10R18: Standard Test Methods for Determining the Izod Pendulum Impact Resistance of Plastics*. West Conshohocken, American Society for Testing and Materials, 2018.

[30] MENEGAZZO, A.P.M., PASCHOAL, J.O.A., ANDRADE, A.M., *et al*., "Avaliação da resistência mecânica e módulo de Weibull de produtos tipo grês porcelanato e granito", *Cerâmica Industrial*, v. 7, n. 1, 2002.

[31] GOULD, R., RYAN, C., *Introductory statistics*, Saddle River, Pearson, 2014.

[32] DEPOY, E., GITLIN, L.N., "Statistical Analysis for experimental-type research", In: DePoy, E., Gitlin, L. N. (eds), *Introduction to research*, 5 ed., chapter 21, Missouri, USA, Elsevier, pp 282–310, 2015.

[33] WASSERTEIN, R.L., LAZAR, N.A., "The ASA statement on p-values: context, process and purpose", *The American Statistician*, v. 70, n. 2, pp. 129–133, 2016. doi: http://doi.org/10.1080/00031305.2016.1154108.

[34] DIRIKOLU, M.H., AKTAS, A., BIRGOREN, B., "Statistical analysis of fracture strength of composite materials using Weibull distribution", *Turkish Journal of Engineering and Environmental Sciences*, v. 26, n. 1, pp. 45–48, 2002.

[35] NOHUT, S., "Influence of sample size on strength distribution of advanced", *Ceramics International*, v. 40, n. 3, pp. 4285–4295, 2014. doi: http://doi.org/10.1016/j.ceramint.2013.08.093.

[36] LU, C., DANZER, R., FISCHER, F.D., "Fracture statistics of brittle materials: Weibull or normal distribution", *Physical Review. E*, v. 65, n. 6, pp. 067102, 2002. PubMed PMID: 12188868.

[37] WOLENSKI, A.R.V., CHRISTOFORO, A.L., LAHR, F.A.R., *et al*., "Estimation of the characteristic tensile strength of the wood in the parallel direction to the grains through of probability models", *Matéria (Rio de Janeiro)*, v. 24, n. 04, 2019.

[38] RABAHI, R.F., LEVY NETO, F., "Analysis of the strength of synthetic marble beams through the statistical distribution of Weibull", *Matéria (Rio de Janeiro)*, v. 21, n. 03, pp. 542–551, 2016. doi: http://doi.org/10.1590/S1517-707620160003.0052.

[39] HANNING, E., GUALBERTO, H.R., SIMÕES, K.M.A., *et al*., "Glass-ceramic produced with recycled glass", *Matéria (Rio de Janeiro)*, v. 24, n. 04, pp. e12505, 2019. doi: http://doi.org/10.1590/s1517-707620190004.0830.

[40] NASCIMENTO, D.C., FERREIRA, A.S., MONTEIRO, S.N., "Weibull analysis of tensile tested piassava fibers with different diameters", *Matéria (Rio de Janeiro)*, v. 23, n. 04, 2018.

[41] QUINN, J.B., QUINN, G.D., "A practical and systematic review of Weibull statistics for reporting strengths of dental materials", *Dental Materials*, v. 26, n. 2, pp. 135–147, 2010. doi: http://doi.org/10.1016/j.dental.2009.09.006. PubMed PMID: 19945745.

[42] KIRTAY, S., DISPINAR, D., "Effect of ranking selection on the weibull modulus estimation", *Gazi University Journal of Science*, v. 25, pp. 175–187, 2012.

[43] DATSIOU, K.C., OVEREND, M., "Weibull parameter estimation and goodness-of-fit for glass strength data", *Structural Safety*, v. 73, pp. 29–41, 2018. doi: http://doi.org/10.1016/j.strusafe.2018.02.002.

[44] PARSONS, F., WIRSCHING, P., "A Kolmogorov - Smirnov goodness-of-fit test for the two-parameter Weibull distribution when the parameters are estimated from the data", *Microelectronics and Reliability*, v. 22, n. 2, pp. 163–167, 1982. doi: http://doi.org/10.1016/0026-2714(82)90174-3.

[45] ANDERSON, T.W., DARLING, D.A., "Asymptotic theory of certain goodness-of-fit criteria based on stochastic processes", *Annals of Mathematical Statistics*, v. 23, n. 2, pp. 193–212, 1952. http://doi.org/10.1214/aoms/1177729437.

[46] WASSERMAN, L., *All of statistics: a concise course in statistical inference*, New York, Springer, 2004. doi: http://doi.org/10.1007/978-0-387-21736-9.

[47] SONJA, E., COUSINEAU, D., "Comparing distributions: the two-sample Anderson-Darling test as an alternative to the Kolmogorov-Smirnov test", *Journal of Applied Quantitative Methods*, v. 6, pp. 1–17, 2011.

[48] YAP, B.W., SIM, S.H., "Comparisons of various types of normality tests", *Journal of Statistical Computation and Simulation*, v. 81, n. 12, pp. 2141–2155, 2011. doi: http://doi.org/10.1080/00949655.2010.520163.

[49] RAZALI, N.M., WAH, Y.B., "Power comparisons of Shapiro-Wilk, Kolmogorov-Smirnov, Lilliefors and Anderson-Darling tests", *Journal of Statistical Modeling and Analytics*, v. 2, n. 1, pp. 21–33, 2011.

[50] SANTOS, F.M., BATISTA, F.B., PANZERA, T.H., *et al*., "Hybrid composites reinforced with short sisal fibres and micro ceramic particles", *Matéria (Rio de Janeiro)*, v. 22, n. 2, pp. e11838, 2017. doi: http://doi.org/10.1590/s1517-707620170002.0171.

[51] SNEDECOR, G.W., COCHRAN, W.G., *Statistical methods*, 8 ed., Ames, USA, Iowa State University Press, 2014.

[52] ROSENBLATT, M., "Remarks on some nonparametric estimates of a density function", *Annals of Mathematical Statistics*, v. 27, n. 3, pp. 832–837, 1956. doi: http://doi.org/10.1214/aoms/1177728190.

[53] BOTEV, Z.I., GROTOWSKI, J.F., KROESE, D.P., "Kernel density estimation via diffusion", *Annals of Statistics*, v. 38, n. 5, pp. 2916–2957, 2010. doi: http://doi.org/10.1214/10-AOS799.

[54] GIBBONS, J.D., CHAKRABORTI, S., *Nonparametric statistical inference*, 5 ed., Boca Raton, Chapman & Hall/CRC Press, 2011.

[55] ARAUJO, E.M., ARAÚJO, K.D., PEREIRA, O.D., *et al*., "Fiberglass wastes/polyester resin composites: mechanical properties and water sorption", *Polímeros*, v. 16, n. 4, pp. 332–335, 2006. doi: http://doi.org/10.1590/S0104-14282006000400014.

[56] BRENES-ACOSTA, A., STRADI-GRANADOS, B.A., "Comparative study of the mechanical properties of polyester resin with and without reinforcement with fiber-glass and furcraea cabuya fibers", *Fibers and Polymers*, v. 15, pp. 2186–2192, 2014.

[57] DEBNATH, K., SINGH, I., *Primary and secondary manufacturing of polymer matrix composites*, Boca Raton, Taylor & Francis Group, 2018.

[58] ARULPRASANNA, A., OMKUMAR, M., "A review on composites: selection and its applications", *Materials Today*, 2024. In press.

[59] MALLICK, P.K., *Fiber-reinforced composites: materials, manufacturing and design*, 3 ed., Boca Raton, CRC Press, 2008.

[60] AFFERRANTE, L., CIAVARELLA, M., VALENZA, E., "Is Weibull's modulus really a material constant? Example case with interacting collinear cracks", *International Journal of Solids and Structures*, v. 43, n. 17, pp. 5147–5157, 2006.